COMPREHENSIVE ANALYSIS OF THE MULTI-BEAM LIDAR SELF-CALIBRATION FOR MOBILE MAPPING SYSTEM

Han Sae Kim (1), Kang Hyeok Choi (2), Yongil Kim (1)

[1] Seoul National Univ., 1, Gwanak-ro, Gwanak-gu, Seoul, 08826, Korea
[2] Myongji Univ., 116, Myongji-ro, Cheoin-gu, Yongin-si, Gyeonggi-do, 17058, Korea
Email: hanswfg@snu.ac.kr; cwsurgy@naver.com; yik@snu.ac.kr

KEY WORDS: Intrinsic Calibration, Velodyne, Point Cloud, SLAM

ABSTRACT: Point cloud acquired by LiDAR (Light Detection and Ranging) sensor inevitably contains errors due to limitations of hardware. In these errors, systematic errors can be specified by photogrammetric calibration which can lead to the improvement of accuracy of the data, providing accurate geometrical features such as planes and lines. On the other hand, recent point cloud registration technique such as SLAM (Simultaneous Localization and Mapping) uses lidar odometry for its front end. Lidar odometry exploits geometrical features of point cloud for its motion estimation when the point cloud is too coarse for point-based feature extraction. Since majority of sensor systems for mobile mapping system uses rotating multi-beam laser scanner which acquires relatively coarse point cloud due to its fixed vertical angle, they hardly provide dense point cloud by on its own. Considering these facts, in this study, to improve the accuracy of point cloud and its geometrical features and improve sensor measurement accuracy, comprehensive analysis of lidar self-calibration was conducted via simulation. Self-calibration was conducted by plane-based model, since conventional method using GCPs (Ground Control Points) cannot be implemented. Self-calibration results were compared in different calibration targets and sensors configurations. With results, we propose a guideline of establishment of calibration dataset to achieve reasonable self-calibration accuracy. Through this experiment, we expect this method to attribute to improve sensor measurement accuracy and geometrical feature in on-site calibration, and data optimization process while registering point cloud data.

1. INTRODUCTION

LiDAR (Light Detection and Ranging) sensor acquires 3D information with high accuracy. In a past decade, the sensor development enabled the use of lidar sensor to various applications such as mobile mapping, Simultaneous Localization and Mapping (SLAM), digital surface model in the field of remote sensing, surveying, and robotics. More recently, the sensor became more portable and compact the more lidar sensor such as Velodyne HDL-64/32E, VLP-16, Hokuyo UTM-10/20/30LX were used for various applications such as mobile mapping system. Multi-beam laser scanner, which Velodyne produces, is one of the extensively used lidar which gives fairly light-weighted, compact, and cheap sensor to interested users. It consists of simultaneously rotating pairs of laser emitters and receivers within compact sensor pod. Majority of mobile scanning related researches uses Velodyne lidar to its sensor system.

In application of autonomous vehicle, five sixth of vehicles that finished the DARPA Grand challenge used Velodyne's HDL-64E. Geiger et al. (2012) acquired and released the popular KITTI dataset for the benefit of community, which acquired its 3d point cloud using Velodyne HDL-64E on moving vehicle platform. On the other hand, Hess et al. (2016) developed its sensor indoor mobile mapping backpack system using VLP-16 as known as google cartographer. Shamseldin et al. (2018) constructed the sensor system using Velodyne VLP-16 for their indoor lidar mobile mapping system. In addition to indoor backpack, autonomous vehicle, or robotic platform, Ravi et al. (2018) mounted Velodyne HDL-32E and VLP-16 on unmanned aerial vehicle (UAV) and developed its mobile mapping system.

Despite its cost-efficient and mobile advantages, the sensor contains systematic errors. Since each mechanically designed multi lasers measure the range by time-of-flight sensor at the same time, point cloud inevitably contains the offsets in range and angle measurements within each laser. These systematic errors can cause translations and rotation of point cloud data. To be implemented in application of mobile mapping, overall accuracy of point cloud expected to be minimized.

In computer vision community, there has been a research to optimize point cloud data to remove undesirable data using RANdom SAmple Consensus (RANSAC) algorithm. Schnabel et al. (2007) proposed RANSAC-based plane detection from point cloud to remove outliers. This data optimization process, however, may exclude inaccurate point cloud, yet remain data still contain systematic errors. To solve this problem and raise the accuracy of point cloud data, sensor calibration process should be pre-performed before its applications.

1.1 Related Work

In surveying community, using photogrammetric technique, there has been extended researches to delineate intrinsic parameters of lidar sensors. Sklaloud and Lichti (2006) first presented rigorous approach to bore-sight self-calibration in airborne laser scanning by conditioning the georeferenced lidar target points to lie on common plane surfaces. In their work, it is more aimed to estimate extrinsic parameters between the IMU and lidar unit, considering only range offset for the intrinsic parameter. It is noteworthy that they also estimated 4 plane parameters within each plane in their adjustment model. Self-calibration analysis on Velodyne HDL-64E was then conducted by Glennie and Lichti (2010) and Muhammad and Lacroix (2010). In Glennie's work, different scan stations with two fixed stations were used to delineate scale parameter. In Muhammad's work, restricted positional conditions were designed to simplify cost function, however this model is not applicable to adjust additional parameters. Gerardo et al. (2011) placed Velodyne-64E in the center of precisely-measured calibration targets. Using pattern planes, they exploited ancillary plane orthogonal distance to minimize planar misclosure using Levenberg-Marquardt algorithm. Chen and Chien (2012) proposed fully-automated on-site recalibration of intrinsic parameters of Velodyne HDL-64E by linearizing the intrinsic parameters. Unlike predominant point-based or plane-based self-calibration methods, Chan et al. (2015) presented a new cylinder-based self-calibration method. The method has more flexibility in terms of geometrical features to condition and avoiding high linear dependencies. Glennie et al. (2016) also conducted calibration and stability analysis of the Velodyne VLP-16 using same mathematical model they used in their previous work.

Overall, using geometrical features such as plane or cylinder with static sensor stations and precisely designed calibration targets, previous studies presented rigorous self-calibration approach to acquire high accuracy 3D information using multi-beam laser scanners. Nevertheless, previous studies were more aimed to develop a static self-calibration approach. Therefore, a careful analysis of self-calibration method for mobile mapping application is needed.

1.2 Purpose of Study

The objectives of this study are: (1) to analyze the effect of using different calibration dataset (i.e., change of calibration targets, sensors, and used points), and (2) to formulate efficient self-calibration method that can be exploited on-site calibration before and during the applications of mobile mapping.

One of the limitations of traditional methods is that they used fixed the position of two or multiple scan station or measured the distance between planes and sensors. These may mitigate the strong correlations among position of station, scale parameter, and orthogonal distance between planes and sensors, yet traditional methods need ancillary data using highly accurate surveying equipment such as total station which hinders the availability of on-site calibration in mobile mapping. Therefore, self-calibration method which does not require any ancillary data needs to be presented for the use of mobile mapping algorithm.

Next, the chance of local optimum can be high in the adjustment for the following reasons. First, the value of parameter estimation through the adjustment expected to be very small and correlations between parameters are relatively high. Second, all points from point cloud can be hardly included in the adjustment due to lack of computer memory. Therefore, self-calibration accuracy may not appear to be stable when it is applicated in different dataset (Glennie et al., 2016). Although estimated calibration parameter may not show the same improvement through all point cloud, it can be applicated in short-term data optimization during mobile mapping algorithm such as SLAM. Knowing the fact that different scan station in conventional static self-calibration method can be roughly interpreted as different frames in mobile mapping, we analyzed the effect of different data acquisition method within expected trajectory to propose short-term self-calibration data optimization method.

Self-calibration and correlation analysis of parameters were performed under simulation. At this stage, mathematical and stochastic models were used which have been well-established and verified in previous studies. The reason for conducting the experiments through simulation is that the simulation test has the following advantages. First, the locations of the lidar and calibration targets can be set to exact values in the simulation. In other words, all the involved orientation parameters can be perfectly controlled in simulation. Contrarily, in the case of self-calibration using real data, there is a limitation in the accurate setting of the positions of the lidar and calibration targets because of an error in the setting of each variable even though it is a sophisticated experiment. Next, simulation can more clearly confirm the accuracy of results than using real data. That is, since the simulation is carried out after setting all the involved variables, the estimated values from self-calibration can be directly compared and analyzed with the preset values. Such comparison is almost impossible in the case of real data. Lastly, simulation can handle different types of calibration targets, lidar orientations without any limitation. Eventually, the results from simulation can reduce the time and economic costs of real experiments (Choi et al., 2019).

In the application of mobile mapping such as SLAM which uses geometrical features to estimate its exterior orientation parameters, we expect this technique to provide accurate such feature by optimizing the point cloud data.

2. MATHEMATICAL MODEL

The mathematical model is based on a functional model which minimizes the misclosure of common planes. This section first introduces ideal system of Velodyne VLP-16, then objective function and stochastic model will be followed. The remainders describe adjustment model that do not require ancillary data such as precisely measured distance between lidar and calibration target to estimate linear scale factor.

2.1 Point Observation Model of Velodyne VLP-16

The Velodyne VLP-16 scanner consist of 16 individual laser emitter and receiver pairs which are individually aimed in 2° increments over the 30° of vertical field of view. The manufacturer defines a set of parameters for each laser to model the deviations from ideal conditions. The computation of cartesian coordinate system is given by:

$$\begin{bmatrix} x \\ y \\ z \end{bmatrix} = \begin{bmatrix} (S_i\, R + D_i)\cos(\alpha_i)\sin(\theta + \theta_i) - H_i\cos(\theta + \theta_i) \\ (S_i\, R + D_i)\cos(\alpha_i)\cos(\theta + \theta_i) + H_i\sin(\theta + \theta_i) \\ (S_i\, R + D_i)\sin(\alpha_i) + V_i \end{bmatrix} \quad (1)$$

where R = raw distance measurement
θ = encoder angle measurement
S_i = distance scale factor for laser i
D_i = distance offset for laser i
α_i = vertical rotation correction for laser i
θ_i = horizontal rotation correction for laser i
H_i = horizontal offset from scanner frame origin for laser i
V_i = vertical offset from scanner frame origin for laser i

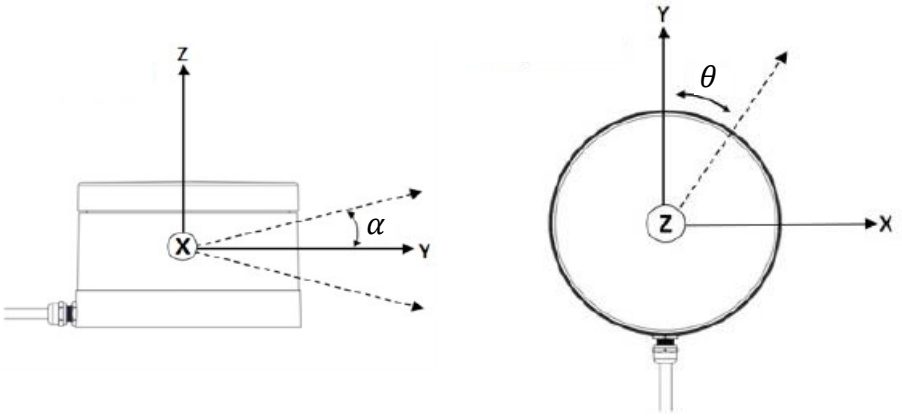

(a) (b)

Figure 1. Coordinate system of the Velodyne VLP-16.
(a) Scanner layout in vertical plane. (b) Scanner layout in horizontal plane.

Among these intrinsic parameters, the horizontal and vertical offset were excluded in our work due to following reasons: (1) calibration parameter are very weakly observable, (2) they are highly correlated to the horizontal and vertical rotations respectively in magnitude between 0.92 and 0.98 (Glennie and Lichti, 2010; Glennie, 2012), (3) physical location of each laser emitter and receiver pair is precisely located from the system CAD drawings, (4) the errors induced by imprecise estimation of horizontal and vertical offset do not depend on the variation in the distance of scanned object (Muhammad and Lacroix, 2010). Therefore, the factory values for these parameters are held as fixed and only four parameters per laser were solved for in the final adjustment.

2.2 Plane-based Functional Model

A plane-based calibration approach presented by Skaloud and Lichti (2006) was implemented in out work, to estimate intrinsic parameters for VLP-16 and plane parameters for calibration targets. The planar observational model is based upon conditioning the lidar returns to lie on common planar surfaces. Since plane parameters are also estimated in adjustment model, true planar surface locations and orientations do not need to be specified in this model. The

functional model for conditioning the points can be expressed as:

$$\langle \overrightarrow{g_k}, \begin{bmatrix} \vec{r} \\ 1 \end{bmatrix} \rangle = 0 = f(\vec{l}, \overrightarrow{x_1}, \overrightarrow{x_2}) \qquad (2)$$

where, $\overrightarrow{g_k} = [g_1\ g_2\ g_3\ g_4]^T$ are the observable parameters of a plane k on which the lidar points are conditioned, $\vec{r}$ is the vector of lidar points within an arbitrarily defined local coordinate system, $\overrightarrow{x_1} = [S_i\ D_i\ \alpha_i\ \theta_i]^T$, and $\overrightarrow{x_2}$ is the vector of plane parameters.

i^{th} point different scan locations, j, can be calculated in a consistent local coordinate frame via a rigid body transformation of the form:

$$\vec{r} = R(w,p,k)_j\ \overrightarrow{l_{ij}} + t_j \qquad (3)$$

where, *R(w,p,k)* and t_j are the rotational transformation matrix and translation vector between the j^{th} scanner space and the locally defined coordinate frame respectively, and $\overrightarrow{l_{ij}}$ is the scanner space coordinates of point *i*, given by Equation (1).

Note that the direction cosines must satisfy the following unit length constraint:

$$g_{1_j}^2 + g_{2_j}^2 + g_{3_j}^2 - 1 = 0 = g(\overrightarrow{x_2}) \qquad (4)$$

2.3 Least Squares Solution

The observations and parameters of the objective function are not separable, and each function includes more than one observation. Therefore, in this study, the combined adjustment model is used. The model minimizes the deviations of the individual lidar points from the planar constraints given by Equation (2). The VLP-16 provides two observations for each point: (1) range, (2) horizontal encoder angle. For each laser, we considered four unknown parameters. Also, point cloud were acquired at unknown location. Therefore, six unknowns for each epoch must be included. In the adjustment of extrinsic parameter, all 16 laser angular offsets cannot be estimated simultaneously. Therefore, reference laser (laser 1) was held fixed. That gives the basic quantities of the least squares adjustment in Table 2.

Table 1. Self-calibration adjustment quantities

# of conditions	m = I
# of unknowns	$u = u_1 + u_2$ = {6*(epochs-1) + 4*(lasers-1) + 2} + 4*P
# of observations	n = 2*I
# of constraints	c = P
# of degrees of freedom	r = I – u + c

The solution to a least squares adjustment of the functional model is described in detail in (Skaloud and Lichti, 2006). The only difference in our work, is that for the purpose of eliminating the need of ancillary data such as precisely-measured calibration target distance from sensor origin or fixed scan station locations, not only plane orientation parameter was treated as weighted parameter, but also the linear scale factor as observable around 1.

3. SELF-CALIBRATION DESIGN

Typically, a higher number of input features and scan stations are needed for the multi-beam laser scanner since the vertical angle of each laser beam is coarsely fixed (Glennie and Lichti, 2010; Chan et al., 2013). Considering their study, before conducting various experiments under different configurations, the minimum conditions of contained planar surfaces to perform reliable calibration should be analyzed. In examining the effectivity of the number of containing planar surfaces, it becomes clear that at least three planes (i.e. ceiling, floor, and wall) should be included in calibration data. Therefore, in this study, four cases of calibration dataset were established to contain at least three common planes. In our experiment, 20m x 10m x 6m of room were set up. Figure 2 describes simulated calibration site and a closer look of planar misclosure due to intrinsic parameters.

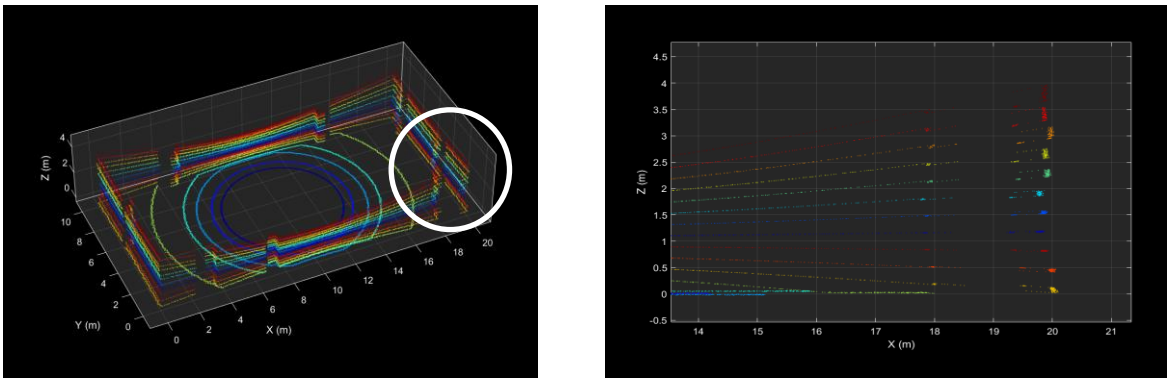

(a) Simulated Calibration Site; Color coded by laser id (b) Planar Misclosure

Figure 2. Simulated Calibration Site and Point Cloud

3.1 Establishment of Calibration Dataset

In this section, four cases of calibration dataset by different sensor position and orientation will be discussed. Assuming mobile mapping system acquires point cloud of simulated room, there are about four cases that can be used as self-calibration dataset.

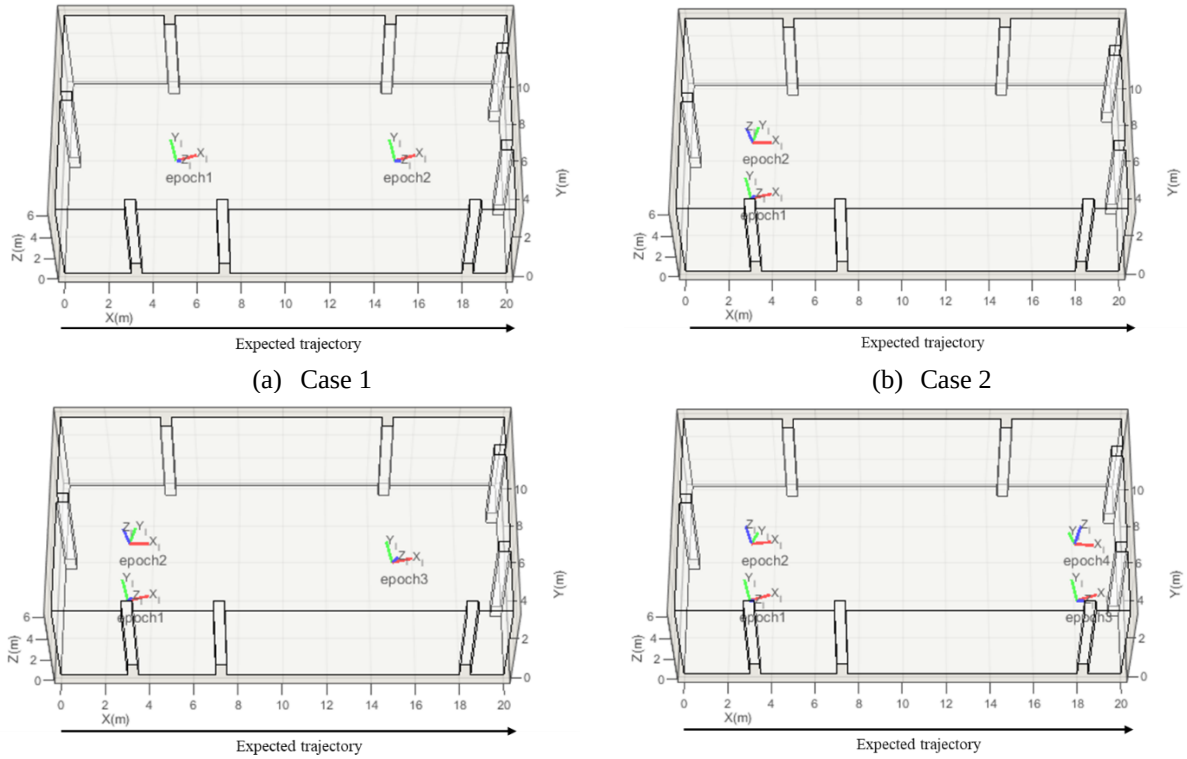

(a) Case 1 (b) Case 2

(c) Case 3 (d) Case 4

Figure 3. Four Cases of Calibration Datasets

Figure 3(a) depicts the sensor configuration along the expected trajectory, while (b) depicts the sensor configuration across the expected trajectory. (c) and (d) are the cases of different combination of (a) and (b). Note that no column planes were included in any calibration dataset.

4. ANALYSIS OF RESULTS

Overall, the geometric calibration of the laser instruments improved the accuracy of the resultant point clouds except for case 3. Calibration accuracy was measured by 1) RMSE (i.e. true error) of range measurement, 2) RMS-residuals

of planar misclosures, and range measurement, and 3) correlations between parameters.

4.1 Planar Misclosure

Since the experiment was conducted under simulated situations, it is possible to compute the true error (RMSE) and residuals (RMS-residuals), respectively. A plot of planar misclosures before and after adjustment is shown in Figure 4 and statistics on the misclosures are given in Table 2.

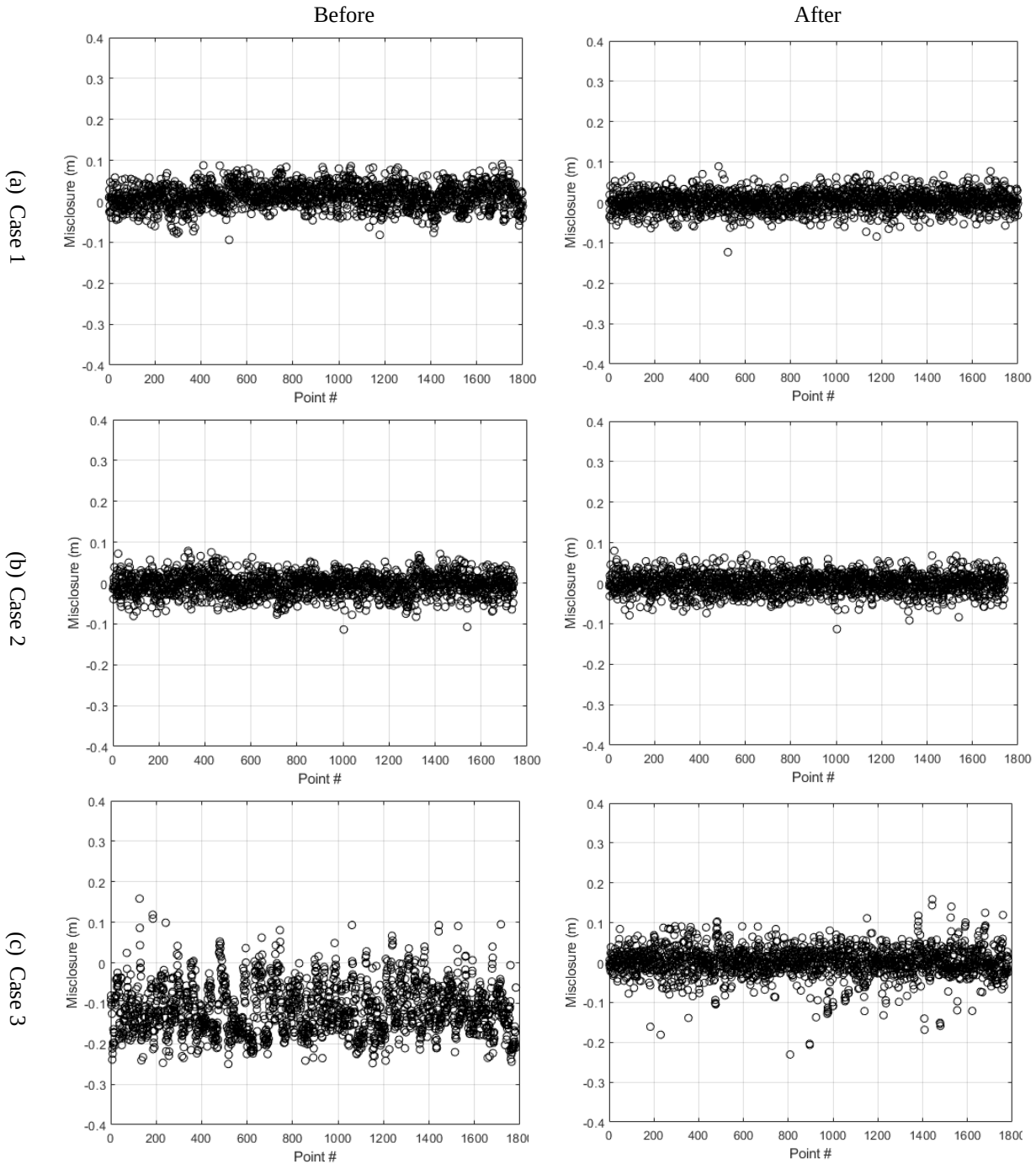

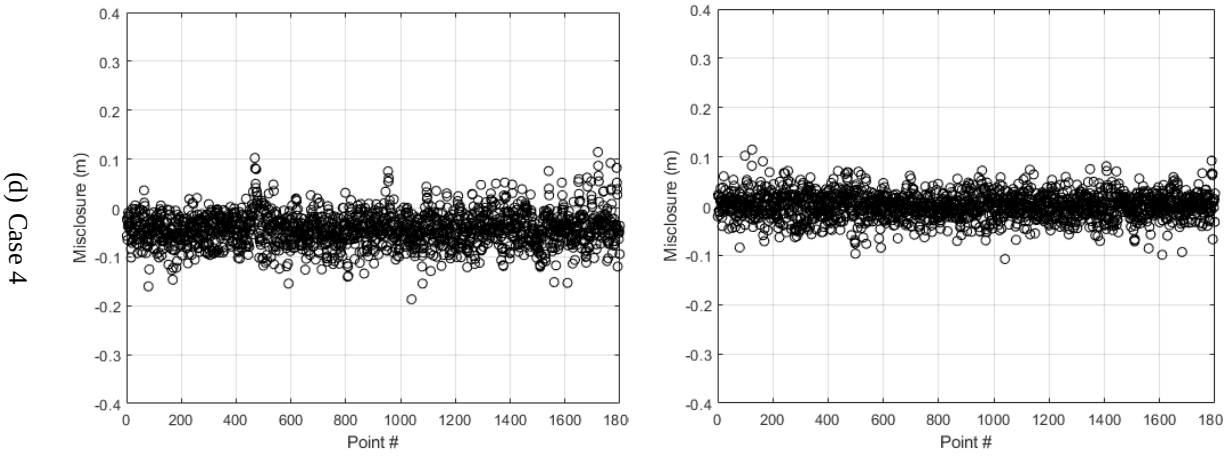

Figure 4. Planar Misclosures Before and After Adjustment within Four Cases

Table 2. Misclosures statistics before and after adjustment

		Planar Misclosure			
Units (m)		Min	Max	Mean	RMSE
Before	Case 1	-0.1397	0.1842	-0.0079	0.0398
	Case 2	-0.1139	0.0786	-0.0042	0.0263
	Case 3	-0.2500	0.1584	-0.1140	0.1296
	Case 4	-0.1867	0.1143	-0.0433	0.0554
After	Case 1	-0.1273	0.0848	0.0001	0.0231
	Case 2	-0.1135	0.0800	-0.0005	0.0240
	Case 3	-0.2307	0.1587	0.0014	0.0373
	Case 4	-0.1074	0.1145	0.0004	0.0261

Examination of the results in Figure 4 and Table 2 shows overall improvement in precision of sensor as a result of the calibration with an exception for Case 3. Among four different cases, Case 4 showed the best improvement comparing to other cases. It is noteworthy that increase of epoch does not necessarily related to increase of accuracy.

4.1.1 Observation Residual

Measurement residuals from the adjustment were also examined in addition to examining planar misclosure. For the measurement, only range data were analyzed for this study. Figure 5 shows plots of the final measurement residual for all points for the least squares adjustment. For the analysis, direct comparison between true range and adjusted range was carried out in favor of simulation experiment.

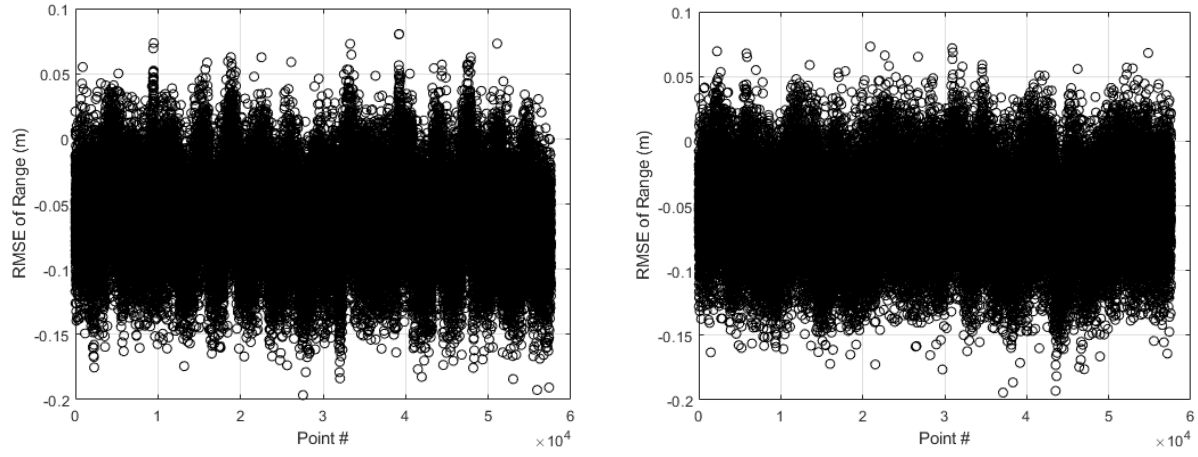

(a) Case 1 (b) Case 2

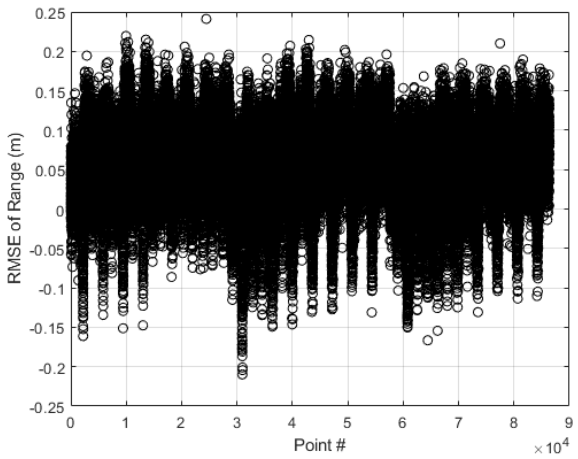

(c) Case 3

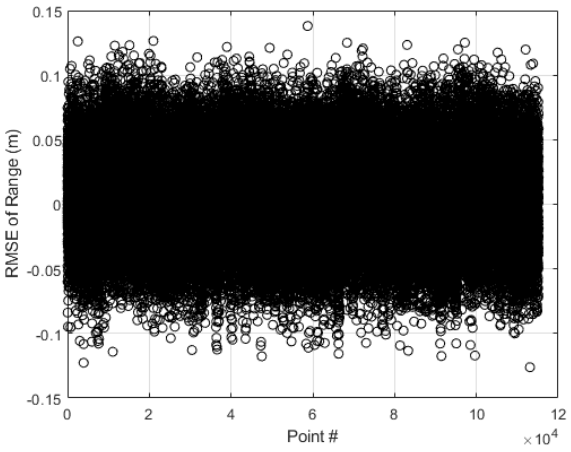

(d) Case 4

Figure 5. RMSE of Range After Adjustment (All Measurements)

For Case 1 and 3, there are still systematic effects since the range residuals do not appear to be normally-distributed. For Case 2, it shows more normally-distributed plot than Case 1 and 3. For the analysis of Case 4, it shows normal distribution, indicating self-calibration was conducted successfully in this case.

Table 3. RMSE of Range Statistics for All Measurements

	RMSE of Range (All measurement)			
Units (m)	Min	Max	Mean	RMSE
Case 1	-0.1627	0.1515	-0.0234	0.0413
Case 2	-0.1943	0.0731	-0.0545	0.0631
Case 3	-0.2098	0.2411	0.0579	0.0759
Case 4	-0.1261	0.1380	0.0064	0.0317

From Table 3, RMSE showed higher value than expected, which is given noise level 0.03m. Case 4 showed the best performance among all cases. Mean value of range residual showed nearly zero in Case 4.

4.2 Parameter Correlation

Correlation between unknown parameters were also examined to measure self-calibration accuracy. As shown in Figure 5, overall strong correlation between scale factor and Xo, Yo, Zo, and d. This is to be expected, whereas there is no network scale constrain excluding the weighted scale parameter for reference laser. Further analysis to decouple correlation among these parameters should be studied.

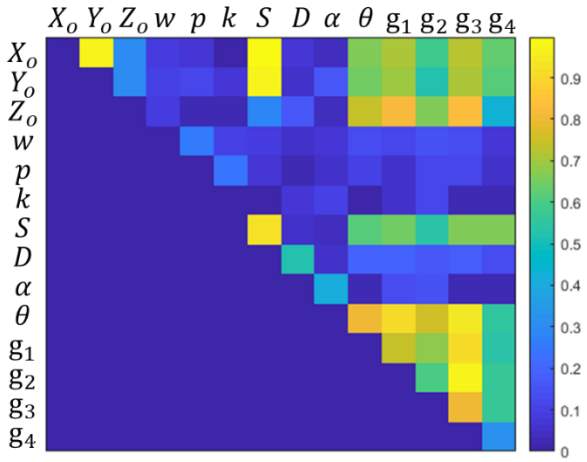

(a) Case 1

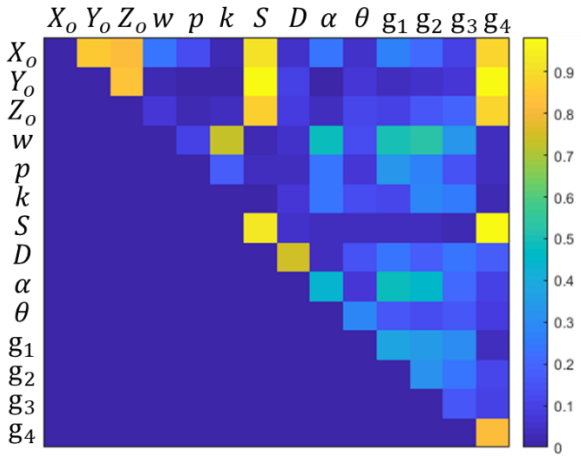

(b) Case 2

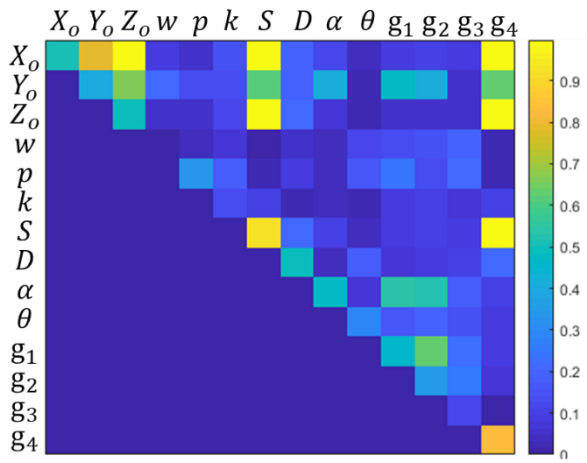

(c) Case 3

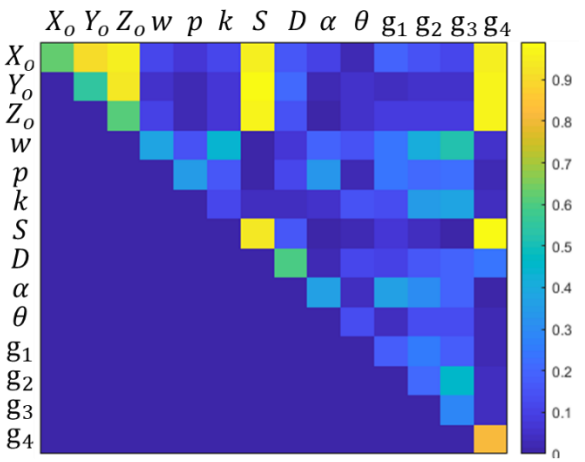

(d) Case 4

Figure 6. Parameter Correlations

4.3 Accuracy of Estimated Parameters

Since the calibration parameters for the laser scanner were solved simultaneously in a least square adjustment, accuracy of estimated parameters can be calculated through error propagation. Table 4 presents the estimated accuracy correspond to each unknown parameter. In case of accuracy of estimated parameter, Case 2 shows the best accuracy of exterior parameters. Further analysis is required for this result.

Table 4. Estimated Parameter Accuracy

	Xo (m)	Yo (m)	Zo (m)	w (deg)	p (deg)	k (deg)	S	D (m)	α (deg)	θ (deg)	g_1	g_2	g_3	g_4 (m)
Case 1	3.0485	0.2310	0.4070	0.0013	0.0005	0.0001	0.0339	0.0060	0.0015	0.1265	0.0005	0.0053	0.0083	1.6625
Case 2	0.0113	0.0807	0.0113	0.0004	0.0001	0.0001	0.0114	0.0031	0.0006	0.0011	0.0000	0.0000	0.0001	0.7199
Case 3	2.5045	0.1586	0.1261	0.0019	0.0010	0.0003	0.0355	0.0088	0.0018	0.0023	0.0000	0.0001	0.0003	2.2526
Case 4	1.9175	0.1007	0.1149	0.0009	0.0004	0.0002	0.0136	0.0033	0.0006	0.0012	0.0000	0.0000	0.0001	0.8772

5. CONCLUSIONS

In this study, we conducted self-calibration with various calibration datasets under simulation. Four different cases were compared to confirm the efficient condition for performing on-site self-calibration and data optimizing. Self-calibration accuracy was measured by examining and analyzing the deviations of parameters, correlations between parameters, RMS-residual of planar misclosure, and RMSE of observations. Overall, self-calibration accomplished improvement of sensor precision. Strong correlation among exterior parameters, orthogonal distance between sensor and planar surfaces, and linear scale factor was examined. In our experiment, Case 4 showed the best performance, achieving RMSE of the range residual in the magnitude of predetermined noise level, while Case 2 showed the lowest average correlations of exterior parameters and the best accuracy.

Nevertheless, our study has following limitations. First, reference epoch should include all planar feature to provide constraints. Such condition has lower chance to be satisfied if the user not acquire point cloud data intentionally. Second, self-calibration accuracy does not appear to be stable when it was applicated to other sets of data. Recalibration must be performed to be applicated other data. To reduce the error in estimation, precisely conditioned calibration should be performed. Lastly, out work needs to be validated in real data.

For future study, different least squares models such as minimizing normal distance of conjugate geometrical features between different scan station will be performed to eliminate the limitations which reference epoch should include all planar features. Moreover, validation of algorithm with real world data will be studied.

6. REFERENCES

Chan, T. O., & Lichti, D. D. (2013, May). Feature-based self-calibration of Velodyne HDL-32E LiDAR for terrestrial mobile mapping applications. In The 8th International Symposium on Mobile Mapping Technology, Tainan, Taiwan (pp. 1-3).

Chan, T. O., Lichti, D. D., & Belton, D. (2015). A rigorous cylinder-based self-calibration approach for terrestrial laser scanners. ISPRS journal of photogrammetry and remote sensing, 99, 84-99.

Choi, K. H., Kim, Y., & Kim, C. (2019). Analysis of Fish-Eye Lens Camera Self-Calibration. Sensors, 19(5), 1218.
Chen, C. Y., & Chien, H. J. (2012). On-site sensor recalibration of a spinning multi-beam LiDAR system using automatically-detected planar targets. Sensors, 12(10), 13736-13752.
Förstner, W., & Wrobel, B. (2004). Mathematical concepts in photogrammetry. Manual of Photogrammetry, 15-180.
Geiger, A., Lenz, P., & Urtasun, R. (2012, June). Are we ready for autonomous driving? the kitti vision benchmark suite. In 2012 IEEE Conference on Computer Vision and Pattern Recognition (pp. 3354-3361). IEEE.
Glennie, C., & Lichti, D. D. (2010). Static calibration and analysis of the Velodyne HDL-64E S2 for high accuracy mobile scanning. Remote Sensing, 2(6), 1610-1624.
Glennie, C. L., Kusari, A., & Facchin, A. (2016). Calibraton and stability analysis of the vlp-16 laser scanner. International Archives of the Photogrammetry, Remote Sensing & Spatial Information Sciences, 40.
Hess, W., Kohler, D., Rapp, H., & Andor, D. (2016, May). Real-time loop closure in 2D LIDAR SLAM. In 2016 IEEE International Conference on Robotics and Automation (ICRA) (pp. 1271-1278). IEEE.
Schnabel, R., Wahl, R., & Klein, R. (2007, June). Efficient RANSAC for point-cloud shape detection. In Computer graphics forum (Vol. 26, No. 2, pp. 214-226). Oxford, UK: Blackwell Publishing Ltd.
Shamseldin, T., Shamseldin, T., Manerikar, A., Elbahnasawy, M., & Habib, A., 2018, SLAM-based Pseudo-GNSS/INS localization system for indoor LiDAR mobile mapping systems. In 2018 IEEE/ION Position, Location and Navigation Symposium (PLANS), pp. 197-208
Velodyne, 2019, Velodyne VLP-16 user's manual. < https://go.pardot.com/l/208822/2018-02-23/6t1jp?File_Name=ManualVLP16&File_Code=ManualVLP16>